AD-A105 530 ROCKWELL INTERNATIONAL THOUSAND OAKS CA SCIENCE CENTER F/G 11/6
MECHANISMS BY WHICH HUMIDITY ALTERS DUCTILITY.(U)
SEP 81 W L MORRIS, M R JAMES, R V INMAN N00014-79-C-0334
UNCLASSIFIED SC5211.2AR NL

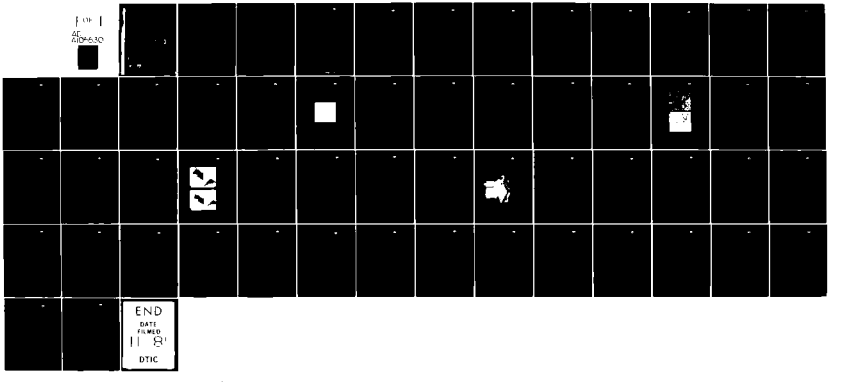

END
DATE FILMED
11 81
DTIC

(12) LEVEL III

SC5211.2AR

Copy No. 86

MECHANISMS BY WHICH HUMIDITY ALTERS DUCTILITY

ANNUAL TECHNICAL REPORT FOR THE PERIOD
April 15, 1980 through April 14, 1981

CONTRACT NO. N00014-79-C-0334

Prepared for

Department of the Navy
Office of Naval Research
Arlington, VA 22217

W.L. Morris
Principal Investigator

SEPTEMBER 1981

Research was sponsored by the Office of Naval Research under contract number N00014-79-C-0334, project number NR036-134 (471).

Rockwell International
Science Center

Unclassified

SECURITY CLASSIFICATION OF THIS PAGE (When Data Entered)

REPORT DOCUMENTATION PAGE

READ INSTRUCTIONS BEFORE COMPLETING FORM

1. REPORT NUMBER	2. GOVT ACCESSION NO. AD-A105 530
3. RECIPIENT'S CATALOG NUMBER	
4. TITLE (and Subtitle) MECHANISMS BY WHICH HUMIDITY ALTERS DUCTILITY.	5. TYPE OF REPORT & PERIOD COVERED Annual Technical Report for the period 4/15/80-4/14/81
6. PERFORMING ORG. REPORT NUMBER SC5211.2AR	
7. AUTHOR(s) W.L. Morris, M.R. James and R.V. Inman	8. CONTRACT OR GRANT NUMBER(s) N00014-79-C-0334
9. PERFORMING ORGANIZATION NAME AND ADDRESS Rockwell Science Center 1049 Camino Dos Rios Thousand Oaks, California 91360	10. PROGRAM ELEMENT, PROJECT, TASK AREA & WORK UNIT NUMBERS NR 036-134 (471)
11. CONTROLLING OFFICE NAME AND ADDRESS Department of the Navy Office of Naval Research Arlington, VA 22217	12. REPORT DATE Sept[illegible] 1981
	13. NUMBER OF PAGES 54
14. MONITORING AGENCY NAME & ADDRESS (if different from Controlling Office)	15. SECURITY CLASS. (of this report) Unclassified
	15a. DECLASSIFICATION/DOWNGRADING SCHEDULE

16. DISTRIBUTION STATEMENT (of this Report)

Reproduction in whole or in part is permitted for any purpose of the United States Government.

DISTRIBUTION STATEMENT A
Approved for public release;
Distribution Unlimited

17. DISTRIBUTION STATEMENT (of the abstract entered in Block 20, if different from Report)

18. SUPPLEMENTARY NOTES

19. KEY WORDS (Continue on reverse side if necessary and identify by block number)

Ductility, surface properties, corrosion environments, fatigue, cracking, fatigue properties, surface defects, crack initiation, aluminum alloys, plastic theory.

20. ABSTRACT (Continue on reverse side if necessary and identify by block number)

The ductility of surface of Al 2219-T851 has been measured in two regimes of plastic strain. In the small strain regime, we determined the microplastic strain which develops within individual grains, at the surface, during fatigue at cyclic stress amplitudes substantially below the bulk yield strength. Initially the deformation is elastic; but, with increasing fatigue, local plastic strains under tensile load develop within individual grains and can approach 0.5%. It is these plastic strains which lead to

DD FORM 1 JAN 73 1473 EDITION OF 1 NOV 65 IS OBSOLETE

Unclassified

SECURITY CLASSIFICATION OF THIS PAGE (When Data Entered)

crack initiation at the surface. The measurement technique is described, and data are presented for two different heats of 2219 taken in dry and in humid air. These materials are thought to differ substantially in as-received hydrogen content. It appears from our results that internal hydrogen increases the rate of development of microplasticity at the surface during fatigue, accelerating crack initiation. The role of surface oxide in determining surface ductility is complex, and is apparently a function of the internal hydrogen content of the alloy. In the large strain regime, the ductility of the surface is assessed by measuring the opening displacements of the tips (CTOD) of small surface cracks. This is done as a function of the distance of the tips to the next grain boundary, so that we can account for the geometric effect of grain boundary constraint on plastic zone size and hence on CTOD. Our results, for three heats of 2219, are consistent with the thesis that at large strains the surface is less ductile in the presence of hydrogen; and that either internal hydrogen or hydrogen extracted from humid air can act to reduce the ductility. Surface ductility measurements are in progress for 2219 specimens charged with hydrogen so that these tentative conclusions can be further tested.

SC5211.2AR

TABLE OF CONTENTS

LIST OF FIGURES

LIST OF FIGURES

LIST OF FIGURES

LIST OF TABLES

ABSTRACT

The ductility of surface of Al 2219-T851 has been measured in two regimes of plastic strain. In the small strain regime, we determined the microplastic strain which develops within individual grains, at the surface, during fatigue at cyclic stress amplitudes substantially below the bulk yield strength. Initially the deformation is elastic; but, with increasing fatigue, local plastic strains under tensile load develop within individual grains and can approach 0.5%. It is these plastic strains which lead to crack initiation at the surface. The measurement technique is described, and data are presented for two different heats of 2219 taken in dry and in humid air. These materials are thought to differ substantially in as-received hydrogen content. It appears from our results that internal hydrogen increases the rate of development of microplasticity at the surface during fatigue, accelerating crack initiation. The role of surface oxide in determining surface ductility is complex, and is apparently a function of the internal hydrogen content of the alloy. In the large strain regime, the ductility of the surface is assessed by measuring the opening displacements of the tips (CTOD) of small surface cracks. This is done as a function of the distance of the tips to the next grain boundary, so that we can account for the geometric effect of grain boundary constraint on plastic zone size and hence on CTOD. Our results, for three heats of 2219, are consistent with the thesis that at large strains the surface is less ductile in the presence of hydrogen; and that either internal hydrogen or hydrogen extracted from humid air can act to reduce the

ductilty. Surface ductility measurements are in progress for 2219 specimens charged with hydrogen so that these tentative conclusions can be further tested.

1.0 INTRODUCTION

Heat to heat variations in the fatigue lifetime of aluminum alloys can be substantial. In high strength alloys, these differences arise both from heat to heat variations in microstructure and from variations in mechanical properties. Crack initiation leading to failure commonly occurs at the surface, and therefore the mechanical properties of the surface, as affected by the ambient environment, are especially important to fatigue behavior. The partial absence of bulk constraint of deformation at the surface, combined with environmental effects, lead to mechanical properties unique to the surface and distinctly different from the bulk. Characterization of these properties requires measurement of the mechanical properties of a very thin layer near the surface. The work reported here deals only with the ductility of the aluminum matrix at the surface, as distinct from effects of environment on constituent particles or grain boundaries. This distinction is fundamental in current development of crack initiation models. In the past two years, under Contract No. N00014-79-C-0334, techniques sufficiently spatially localized to measure matrix ductility within individual grains have been developed, and five parameters have been identified which describe various aspects of the microplastic deformation behavior of a surface.[1] Heat to heat variations in these parameters have been measured in Al 2219-T851 alloys, which are sufficiently large to have a substantial effect on fatigue lifetime. Our experiments suggest that the most important variable in material composition, from heat to heat, which affects the mechanical

properties of the matrix material at the surface is the internal hydrogen content of the alloy.

Our present model of the surface ductility of aluminum envisions a complex interaction between the surface oxide, internal hydrogen and hydrogen liberated from water vapor by surface oxidation. The evidence for this is discussed in Sections 2.0 and 3.0. Testing of this model requires the measurement of the surface ductility parameters as a function of alloy hydrogen content. This work is currently in progress.

An especially important distinction which must be drawn is between the effect of hydrogen on small microplastic surface strains which leads to crack initiation, and of hydrogen on microcrack tip plasticity which affects closure stress and thus influences crack growth rate. It appears that at small strains hydrogen enhances plasticity and accelerates crack initiation, for several aluminum alloys. For large plastic strains, such as experienced at crack tips, hydrogen in Al 2219-T851 reduces plasticity, decreases the closure stress and accelerates crack growth rates. While internal hydrogen can affect both initiation and early growth, it appears that environmental hydrogen alters only crack growth in Al 2219-T851. This is possibly because the hydrogen atom does not penetrate the surface oxide of specimens fatigued, at small plastic strains, in laboratory air.

2.0 BACKGROUND AND RECENT RESULTS

Environmental humidity can have a significant effect on the fatigue lifetime of aluminum alloys and a controversy still exists over the source of this effect. Many years ago, Grosskreutz[2] demonstrated for pure 1100 aluminum that the surface oxide thickness and mechanical strength affected the near surface dislocation structure developed during fatigue. Thicker and more adherent oxide limits dislocation motion through the surface and leads to trapped dislocations and tangles near the surface. Critical strains for oxide fracture measured by Grosskreutz are approximately 0.05%, however. The aluminum alloys of interest to us have much higher yield strengths than Al 1100 and hence are subjected to peak surface strains approaching 0.5% during fatigue. The surface oxide of 2000 series aluminums must be grossly fractured by fatigue. Nevertheless, TEM studies of near surface dislocation structure in Al 2024-T3, done under the present contract,[1] show the same trends as reported by Grosskreutz. In dry air, dislocation structures were banded after substantial fatigue, while in moist air there were tangles of dislocations near the surface. One can postulate that reoxidation during fatigue in moist air maintains sufficient oxide adherence to affect dislocation motion through the surface. Also, recent research by Viswanadham et al.,[3] has shown that the composition of the surface oxide responds to small changes in alloy chemistry. Thus there is prospect that alloy composition can effect fatigue properties through surface oxide composition and the concomitant mechanical properties of the oxide. Hardwick et al.,[4] have demonstrated

that hydrogen charging will reduce the fatigue lifetime of 7000 series aluminum, even in the absence of a transition to the intergranular fracture mode that can occur in the zinc containing 7000 series materials. While it is possible that this change resulted from modification of the near surface microstructure during charging, a direct effect of hydrogen on the alloy matrix is probably involved. It has long been argued that surface oxidation in the presence of water vapor will provide a source of hydrogen at the alloy surface, and hence the effect of moisture on the fatigue lifetime of aluminum may simply be due to hydrogen embrittlement. On careful examination, however, this simple model is not persuasively sustained. Two phases of the fatigue failure of aluminum must be distinguished, crack initiation and early crack growth.[5-7] During fatigue at stress amplitudes below the alloy yield strength, crack initiation involves only very small microplastic strains at the surface, and humid air typically increases the duration of time to initiation. Once surface cracks have developed, crack growth rate is substantially faster in humid air due to a lower ductility of the material at the surface crack tips. Thus, moist air typically decreases the ductility of the surface of aluminum for both small strains (initiation) and large strains (crack growth). We present evidence here, however, that hydrogen increases the ductility of the matrix material at the surface, for small plastic strains.

The research reported here concerns the surface ductility of three heats of Al 2219-T851 with nominally the same composition, within the ranges indicated in Table 1. As shown, the three heats identified, I, II, and III differ principally in Fe content over a range of a few tenths of a percent,

and we believe in hydrogen content. Commercially measured hydrogen contents are less than 1 part per million for these materials, and are therefore too small to be relied upon. Instead we have employed bubble counting in annealed specimens to obtain a qualitative comparison of the hydrogen contents. This procedure and the development and evolution of a hot salt bath technique to charge samples of Al 2219-T851 are discussed in Section 2.1. Experimental results on surface ductilities of the alloys at low plastic strains affecting initiation, and at high strains affecting early growth are discussed in Sections 2.2 and 2.3 respectively.

Table 1
Chemical Composition of Al 2219-T851 Alloys

	Heat I %	Heat II* %	Heat III* %
Silicon		0.05	0.07
Iron	<0.01***	0.22	0.14
Copper		6.02	5.94
Manganese		0.29	0.31
Magnesium		0.008	<0.001
Zinc		0.04	0.03
Titanium		0.07	0.04
Vanadium		0.13	0.11
Zirconium		0.18	0.15
Oxygen		0.0031	0.0024
Nitrogen		0.003	0.001
Hydrogen	Medium**	High**	Low***

*Data from Luvak, Inc., Boylston, MA.
**All less than 1 ppm. Ranking by bubble densities.
***Special low Fe alloy.

2.1 Hydrogen Content and Hydrogen Charging of Aluminum

The typical hydrogen content of as-received aluminum is less than one part-per-million and is difficult to measure with accuracy. The hydrogen content of aluminum can differ substantially from heat-to-heat, however, in part in response to the amounts of scrap aluminum used in forming the melt. Potentially, the most accurate method to measure hydrogen content is to melt a sample and collect and analyze the gas given off. Small amounts of adsorbed water and hydrocarbons on the specimen surface can provide sufficient hydrogen to mask the internal hydrogen, however, and very careful specimen preparation is required. Additionally, this technique of necessity measures all the hydrogen present and can not distinguish the microscopic sites of location of the hydrogen. We have used instead a qualitative technique to determine internal hydrogen content in our aluminum materials, which we ultimately plan to calibrate. The method was suggested by Cliff Bampton at the Science Center and is based upon a methodology developed by investigators fifteen years ago.[8,9] Specimens to be characterized are annealed at 515°C to produce internal bubbles in the material. The specimen is then sectioned and polished so that bubble sizes and total volume can be determined. Heavy anodizing prior to annealing limits hydrogen transport through the surface. In the absence of anodization, hydrogen loss results in production of a peak density of bubbles some hours after annealing begins, the actual time of which is dependent upon specimen thickness and annealing temperature. The peak is found by taking data for a sequence of specimens annealed for progressively longer times. We used this approach for Al 2219-T851 specimens 0.25 cm thick,

and found the most and largest bubbles were formed after 3 hours at 515°C. The difference in bubble size distribution between heats II and III (ref. Table 1) are illustrated in Fig. 1.

The bubbles we observe are typically nucleated at constituent particles, such as seen in the micrograph in Fig. 2. These can be confused with artifacts arising from polishing, unless the researcher has spent some time becoming experienced with the polishing characteristics of his materials. We find that pitting arising from both localized corrosion and from embedded polishing particles can be mistaken for bubbles, especially if the bubbles are counted using optical microscopy. These artifacts can be completely eliminated by prolonged polishing of specimens with Al_2O_3 powders, decreasing in size, and ending with a 0.05 μm powder. We tried kerosene as a working fluid and never achieved a satisfactory looking polish. The best and most consistent results were achieved with water as the working fluid using a felt cloth mounted on a glass insulated polishing wheel to prevent corrosion while polishing. Specimens were immediately rinsed with acetone, after polishing and while still wet, to prevent corrosion pitting that can result if water is allowed to dry on a specimen. Bubble densities obtained were quite reproducable with this procedure.

Bubble density characteristics have been studied extensively for Heats II and III, for which the majority of our surface ductility data have been obtained. Bubbles are found in both materials prior to annealing and are a function of depth below the surface of the plate stock. Data for the two heats are illustrated in Fig. 3. We think it likely that the variation in

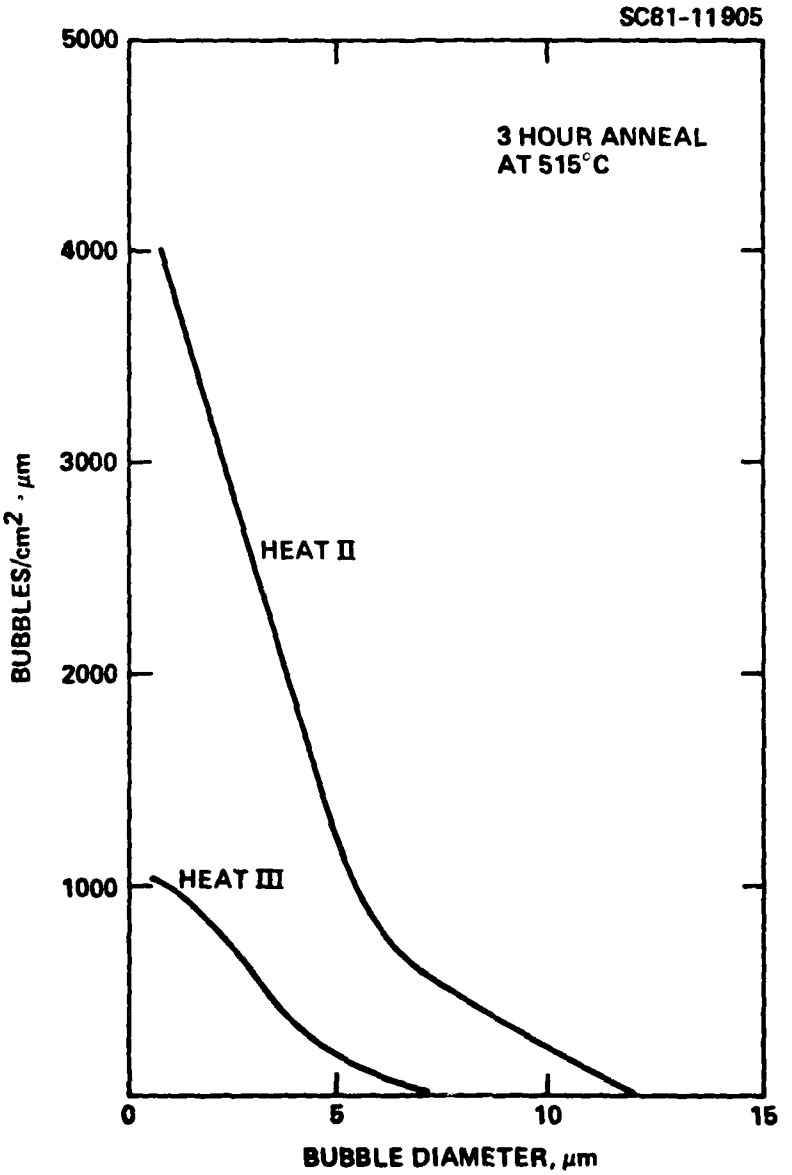

Fig. 1 Histogram of the diameter of bubbles sectioned at the surface of specimens taken from the center of the plate stock for Heats II and III. Specimens annealed for 3 hours at 515°C.

SC81-14401

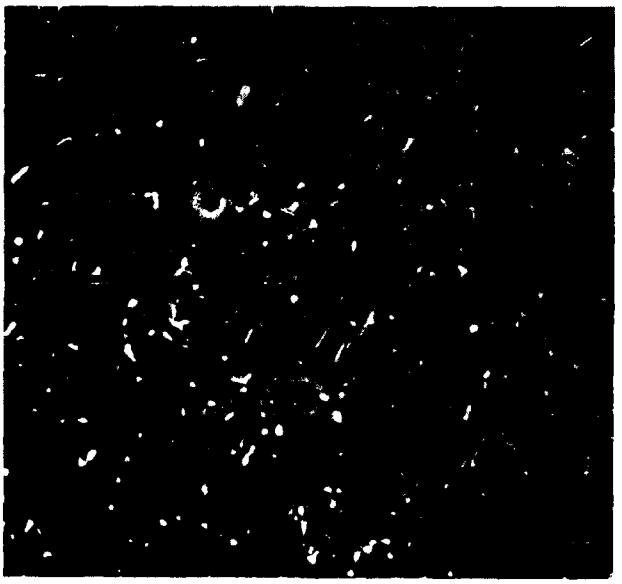

Fig. 2 Scanning electron micrograph of voids at constituent particle sites in Heat II. These are typically hemispherical, suggestive of bubbles. Bar is 10 μm.

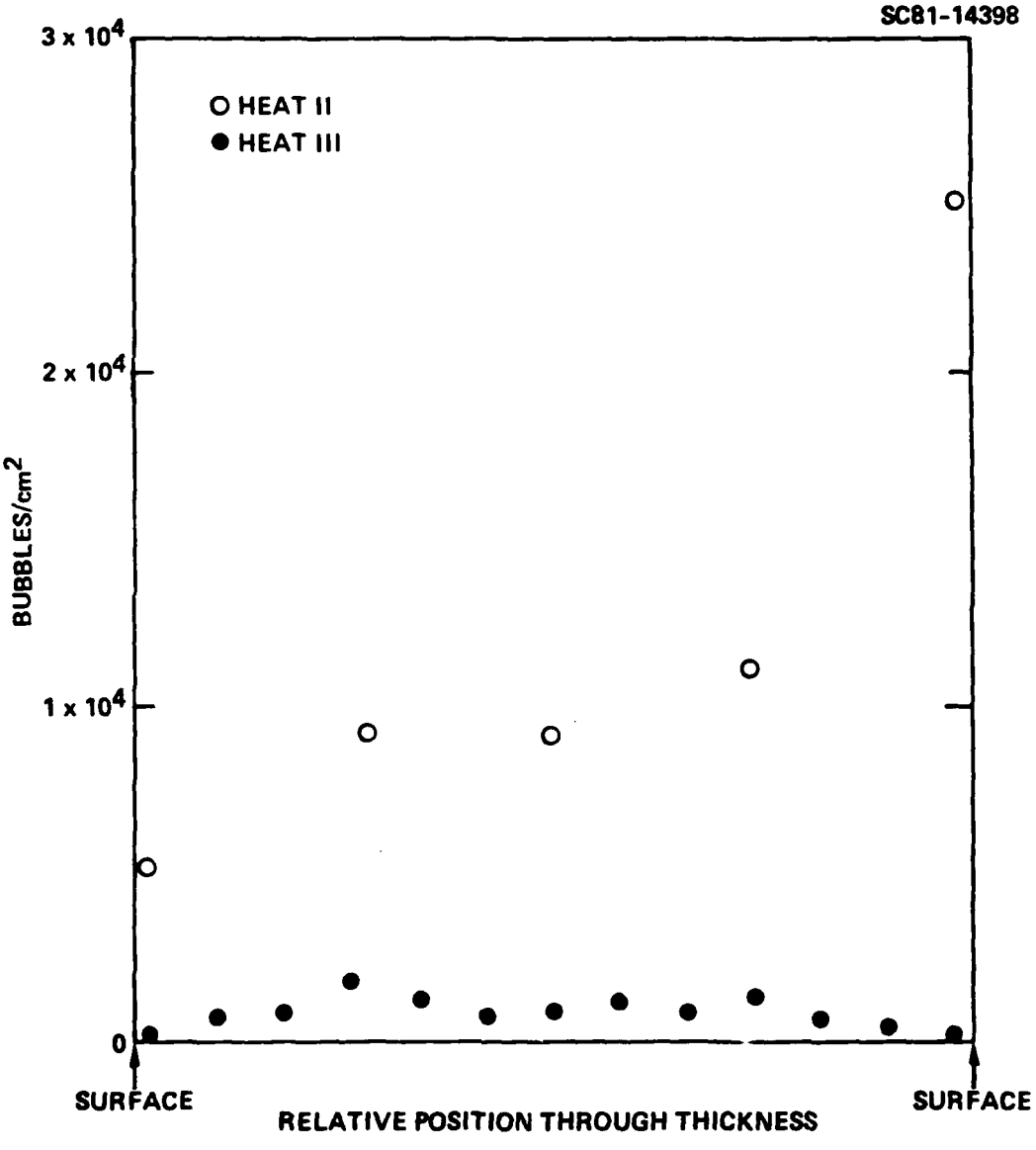

Fig. 3 Distribution in numbers of bubbles/cm^2 sectioned as a function of depth below the surface of the as received plate stock, for Heats II and III.

bubble density with depth does not indicate a variation in hydrogen content with location in the plate, but instead a variation the numbers of sites at which hydrogen is easily precipitated. For this reason we can not yet be certain that Heat III contains less hydrogen than does Heat II. However, we find that, by hydrogen charging Heat III, we can increase the bubble density after annealing to approximately that found for Heat II. This further suggests that Heat III contains less hydrogen than II in the as-received state. In general we find that bubble density increases slightly with annealing up to three hours, and thereafter decreases. The relative ranking of hydrogen content given in Table 1 for the three heats, is obtained from a qualitative comparison of the numbers of bubbles on specimens in the as-received condition.

Aluminum is somewhat tricky to charge with hydrogen, because the surface oxide is a good barrier to hydrogen transport. We have had considerable success however, using a modified form of the hot salt technique, initially developed by Elkholy[10] to hydrogen charge difficult materials. Specimens are charged using the apparatus illustrated in Fig. 4. The salt bath consists of $NaHSO_4$, $KHSO_4$ and Na_2SO_4 in the proportions (37.55/42.5/16) by weight. Sufficient water is then added to melt the salts at temperatures above 150°C. The maximum possible operating temperature in our apparatus decreases as more water is added, due to evaporation cooling. The water must be replenished for hydrogen charging to continue. We initially tried using a steam bubbler to continually resupply the bath with water as recommended by Elkholy. This never worked satisfactorly. Commonly, we found the specimen

SC81-14399

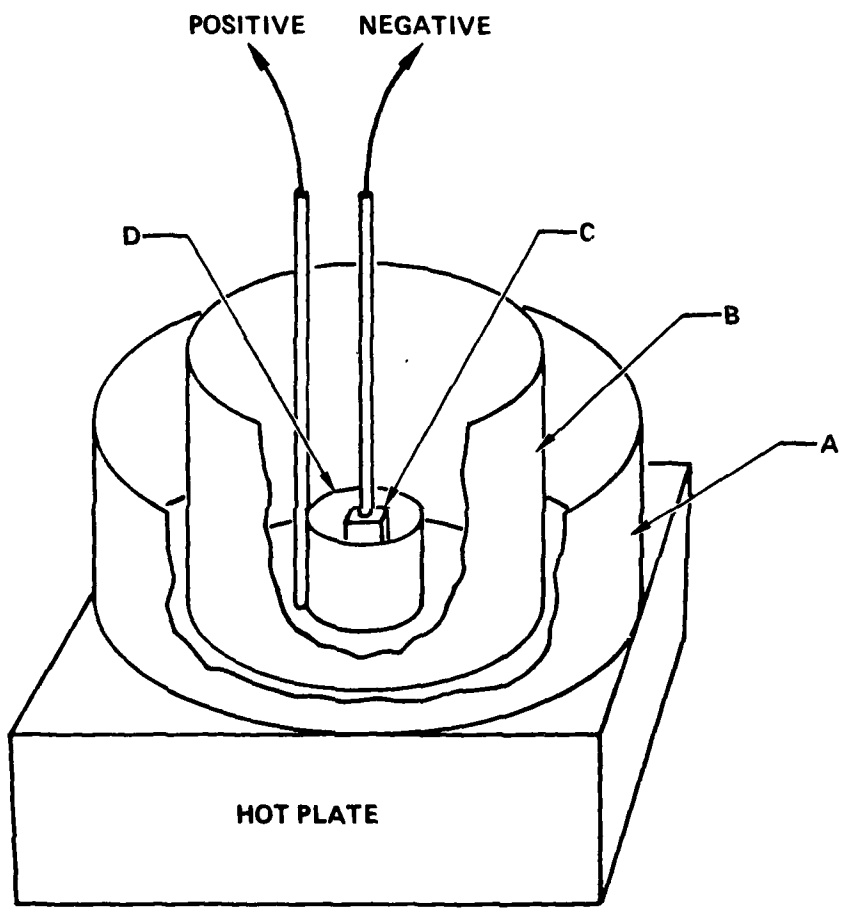

Fig. 4 Schematic drawing of the salt bath apparatus used for hydrogen charging: (A) outer quartz beaker containing diffusion pump oil; (B) inner quartz beaker containing salt; (C) specimen; (D) platinum anode. Not shown is that the charging beaker is also covered by a watch glass.

incrusted in a red oxide, and on post annealing found no indication that hydrogen had entered the bulk. Instead, we had repeated success by operating the bath with sufficient water content to maintain a 170°C operating temperature. Water was added by hand every hour by pouring a few drops directly on to the hot salt, well away from the specimen. This is not a procedure we would recommend to anyone else. No problems with splattering hot salt or breakage of the quartz container has been encountered, but the potential is there and the procedure must be approached with extreme care.

Charging currents of approximately 0.2 amps/cm^2 were maintained, and the voltage between the specimen and platinum anode was allowed to vary freely. Values between 3 and 12 volts were commonly observed for our experiment, with the voltage increasing as water evaporated from the bath. No more than four hours was required to saturate Heat III with hydrogen. A lower bound on the time for an adequate charge remains to be established. We have been able to charge 1/4 in. diameter bars of Mar-M-246 to 10 parts-per-million in two hours, however. This suggestes that a very brief exposure of aluminum to the charging bath might be sufficient for our purpose.

The surface of Al 2219-T851 is severely corroded during charging, leading to reduction in thickness in some places of as much as 0.004 cm. However, the amount of thickness change in charged specimens can vary substantially from run to run. The reason for this difference, and its possible relationship to success in charging, remains to be determined. The grain boundaries of charged specimens were observed to be slightly etched after charging. When these specimens were then annealed sufficient hydrogen

evolved at the boundaries to actually lift some of the grains out of the surface (Fig. 5). Heat III specimens polished to remove 0.007 cm of material before annealing show increases in bubble densities of almost an order of magnitude, and no grain boundary fracture. Control specimens placed in the bath but not in the charging loop did not show these changes, but are of course vulnerable to some alteration in mechanical properties due to the exposure to a 170°C annealing temperature. We hope that the restriction of our research to overaged materials and short charging times will minimize this problem.

2.2 Measurement of Surface Ductility at Low Plastic Strains

During fatigue at cyclic stress amplitudes well below the yield strength, the mechanical properties of the surface of Al 2219-T851 changes progressively. As measured by microindentation hardness, the surface cyclically hardens as is common for aluminum alloys.[11] In fact, as shown in Fig. 6, we find the matrix material hardens most in the largest grains.

However, in an apparent contradiction, the local yield strength within individual grains initially decreases during fatigue as described in Section 2.2.2. It is the resulting microplastic strain at the surface that is responsible for crack initiation at constituent particles in the alloy. A technique to measure the cyclic plastic strains developed when an alloy is fatigued below its bulk yield strength was developed under Rockwell IR&D funds and is described in Section 2.2.1. Results obtained using the technique under this contract are given in Section 2.2.2. We defer discussion of our

SC81-14400

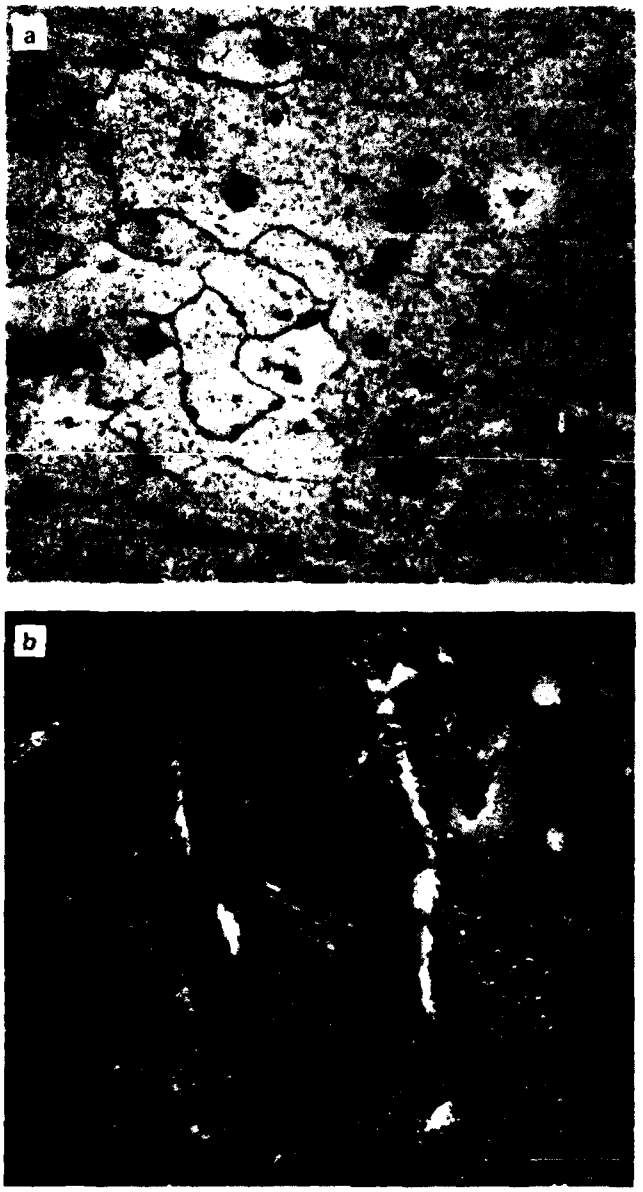

Fig. 5 Micrograph of the surface of the Heat III after hydrogen charging and after a 3 hour anneal at 515° C, showing damage to grain boundaries; (A) optical at 250X, the pits are at the sites of constituent particles etched out during charging; (B) scanning electron micrograph showing lifting of grain out of the surface (bar is 10 μm).

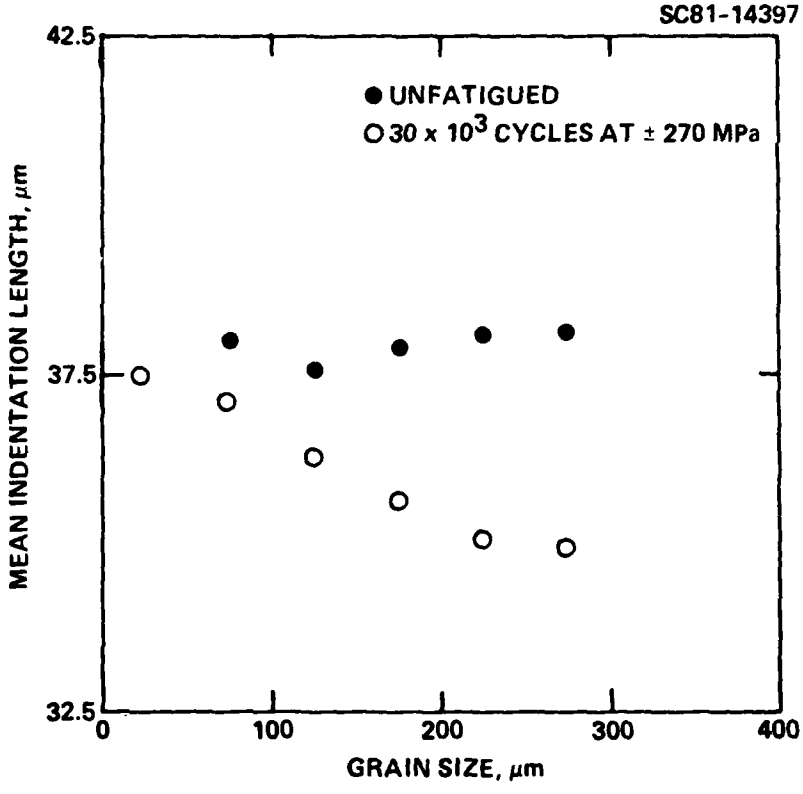

Fig. 6 Indentation hardness of Heat III as a function of the diameter of the grain indented. Measured using 10 gm Knopp indenter. Data presented is the length of the indentation and is the mean of appoximately 7 (substantially scattered) measurements for each grain size. Indentation length decreases with hardness. The effect of fatigue is to increase the surface hardness preferentially in the largest grains.

rationalization of the simultaneous manifestations of hardening and of softening of the surface of Al 2219-T851 during fatigue to Section 3.0.

2.2.1 The Measurement of Surface Microplasticity Within Individual Grains (Rockwell International Funded Research)

For fatigue at stress amplitudes substantially less than the alloy yield strength, plastic slip near the specimen surface is blocked by the grain boundaries.[6,12,13] Crack initiation is attributable to a progressive increase in localized microplasticity within individual grains.[14,15] Models of this process are commonly divided into two sequential parts. First, the peak tensile plastic strain produced within an individual grain, on each loading cycle, is predicted with an appropriate model of mobile dislocation development. Next, an initiation criterion is employed to relate the probability of crack formation to the type, geometry and mechanical properties of the site of weakness within the grain and to the peak plastic strain of the matrix material within the grain. It is the properties of the matrix which we seek to understand.

Such models can in principle be validated by comparing predicted and measured rates of crack initiation. If disposable model parameters limit the sensitivity of such evaluations, the model describing microplasticity can instead be tested by directly by measuring the amount of fatigue induced plastic strain within individual grains. In this section, we describe a technique to make such measurements which has several advantages over other methods used to obtain similar or related data.

In essence, we use a small (~ 20 μm) flake of mica located within a grain of interest as a reference gauge and measure strains in the surface relative to this gauge in a scanning electron microscope (SEM). This method is more accurate for measuring small plastic strains than selected area backscatter electron channeling[16] or stereoimaging,[17] which are best suited to measure plastic strains larger than 0.5%. It also avoids the interpretive problem encountered with channeling, where one must calibrate plastic strains using uniaxial loaded specimens. The sensitivity to measure deformation at the surface with a reference gauge appears to be comparable to that obtained by Pangborn et al.[18] with their use of using X-ray double crystal diffractometry, but the reference gauge data are obtained directly in terms of local strain and are simpler to relate to current initiation models. The reference gauge method permits crack initiation models to be evaluated by measuring peak strains in preselected grains containing potential initiation sites of interest.

The capabilities and limitations of the technique are described. Results are presented for an Al 2219-T851 alloy for which progressive fatigue at stress amplitudes below the yield strength produces increasing plastic strain at the surface, with preference for development of the largest plastic strain in the larger grains. Elastic strains in the smaller grains at the surface are shown to be driven into compression during unloading to accommodate these changes.

The strain measurement technique, illustrated in Fig. 7, utilizes as a reference gauge a flat particle of mica lying on the specimen surface within

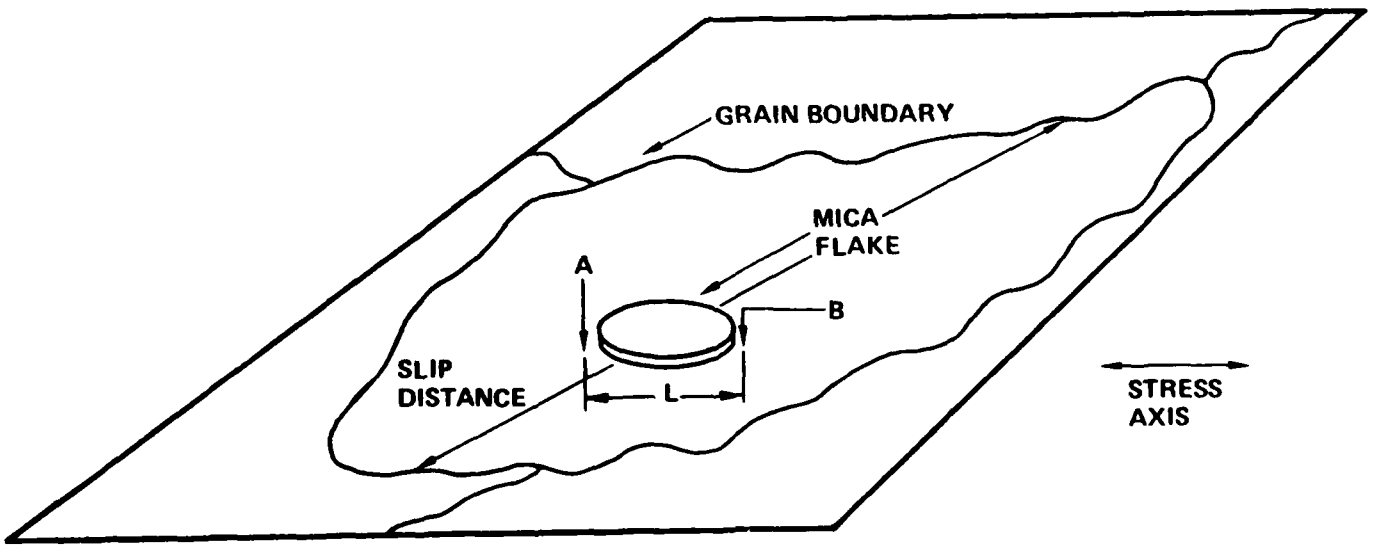

Fig. 7 The reference gauge technique. The mica flake lies within a grain and is not bonded to the substrate. Strain over the gauge length L is determined by measuring the locations of points A and B, before and after loading, relative to the mica. The maximum slip distance D, plotted in Fig. 11, is the larger of the two grain widths through the mica flake, measured at a 45° angle to the principal stress axis.

a grain. We measure the distance L between points A and B on the substrate at zero externally applied stress and then load, in the microscope, the surface through a tensile cycle returning to zero applied stress. The new distance L' between A and B is then determined and the residual cyclic strain parallel to the principal stress axis is defined as

$$\varepsilon = \Delta L/L = (L' - L)/L \quad . \tag{1}$$

The measurement thus determines the width of the stress-strain hysteresis loop at zero external load. If ε is different from zero, local yielding has taken place, although not necessarily within the grain of measurement. ε is the sum of the local plastic strain and the internal elastic strain necessary to accommodate yielding in surrounding grains.

The mica flake provides a reference which substantially increases the accuracy of the measurement of ΔL. High resolution SEM micrographs are obtained which show both the substrate and the mica edge (Fig. 8). Such micrographs taken before and after loading at each point A and B are then observed with a stereoscopic viewer. A small relative displacement in position between the mica and substrate in the before and after loading pairs causes the edge of the mica to appear to lie at a different depth than the substrate. Displacement of the substrate relative to the mica can accurately be determined with a floating point device such as in common use in aerial mapping (Fig. 9.). The apparent height of the arrow above the substrate is a function of the true distance between the arrows under the viewer. The

SC81-13983

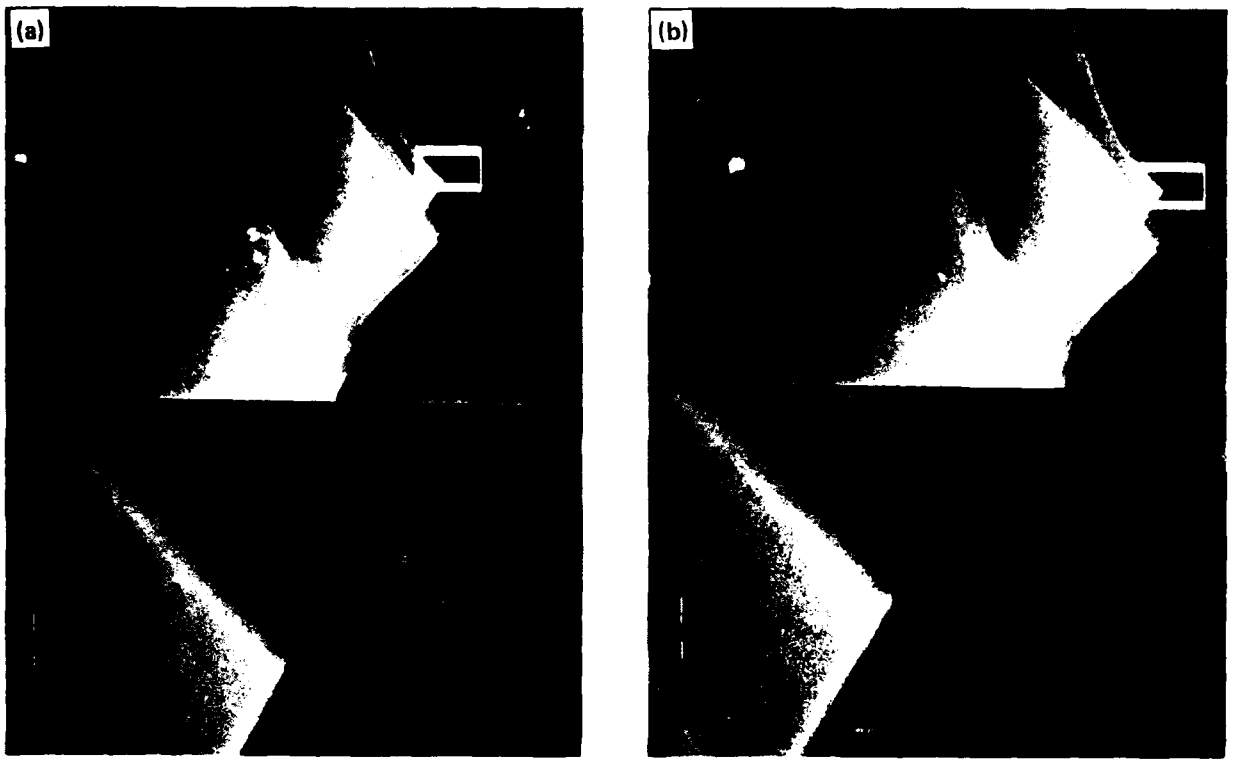

Fig. 8 Typical micrographs of an area near the edge of a mica flake; a) before loading, b) after loading. Dual magnification is used to facilitate relocation of the measurement point after loading with the low magnification half at 3000 X and the high magnification half at 30,000 X. The mica edge is to the left in all views. The substrate in (b) is 580Å further to the right of the mica than in (a). The shift is much easier to see when the pair of micrographs are viewed stereoscopically.

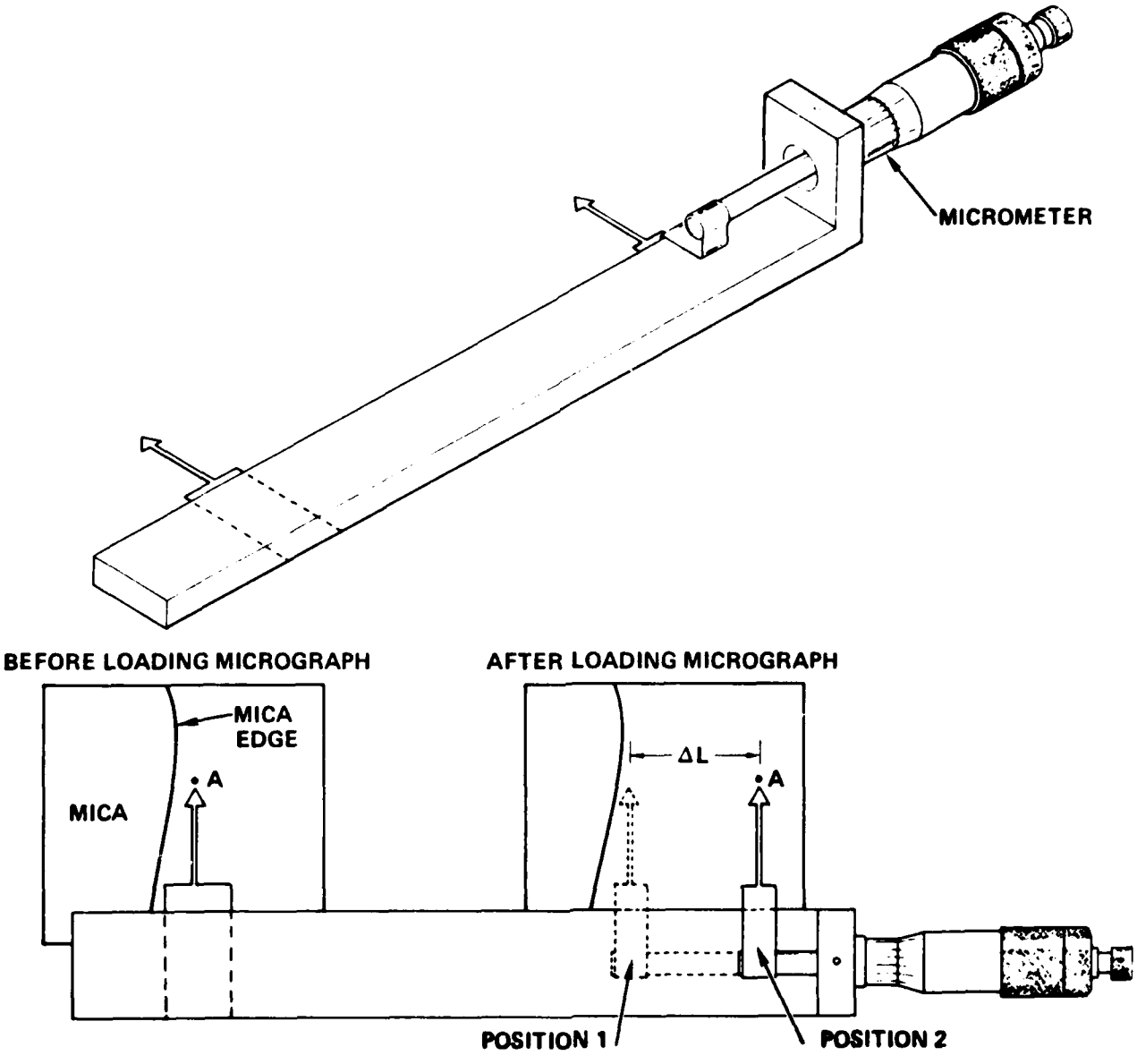

Fig. 9 A floating point device as pictured in (a) is used to measure displacement of the substrate relative to the mica. The pointer on the left is fixed while that on the right moves laterally by turning the micrometer. The observer places the instrument over the two micrographs (before and after loading at the same position, either A or B) and using a stereoscopic viewer, adjusts the traveling pointer so that it first appears to lay at the height of the substrate. This is illustrated in (b) as position 2 (point A on the substrate has moved during the loading cycle). The traveling pointer is then adjusted so that it appears to lie at the same height as the mica (position 1). The linear displacement read on the micrometer is ΔL at point A. Accuracy in the measurement of ΔL is substantially improved by stereoscopic viewing.

observer adjusts the traveling arrow so that it first appears to lie at the same depth as the substrate, and then at the same depth as the mica, and records the linear displacement of the traveling arrow by using a micrometer. ΔL is the sum of the linear displacements at points A and B. The human eye uses the entire image to make apparent height decisions and the resulting sensitivity in measurement of displacement can be substantially better than that obtained from direct measurements off the micrographs. With good micrographs the statistical scatter from repeated measurements in displacement obtained with our equipment is $\pm.005$ cm. Using micrographs taken at a magnification of 35×10^3, we can measure ΔL to ± 20 Å. The resulting sensitivity in strain is, of course, a function of the gauge length, L. Strains of 0.01% ± 0.005 can be measured within individual grains with optimum microscope resolution.

There are several tricks to make this technique work well. Mica flakes in a size range of 15 to 60 μm can be prepared using a rotating blade glass cutter to crush mica in a mortar. The best flakes are very thin and flat so that they maintain close contact with the substrate, and thus both the mica edge and the substrate can be brought into simultaneous focus in the SEM. An added advantage of thin, flat mica flakes is that they are less likely to tilt relative to the substrate as a result of the loading. Such movement would introduce error into the strain measurement. In our experience, tilting occurs for about one particle out of 20 and is easily recognized, since different points on the mica edge appear to lie at different heights. There is no accurate way to correct for tilting and data from such

particles are not used. It is not necessary to coat the mica particles to prevent charging in the SEM, but stigmation of the electron beam in the vicinity of a particle measurement site is advisable.

Tapered cantilever flexural fatigue specimens were prepared from rolled plate stock of Al 2219-T851 with the specimen surface in the rolling plane and with the principal stress axis parallel to the rolling direction. The mean grain size in the rolling direction was 100 μm and in the long transverse direction was 75 μm. The alloy yield strength was 360 MPa. The specimens were machined with progressively decreasing cutting depths to minimize residual surface stresses. They were mechanically polished ending with 0.05 μm Al_2O_3 powder and chemically etched to reveal the grain boundaries. Residual stress measurements using X-ray diffraction indicated all samples were within ±20 MPa of being stress free.

The specimens were fatigued in dry air in flexure, using stroke control and fully reversed loading (R = -1), and were then lightly dusted with mica flakes. Flakes within grains of interest were located by optical microscopy (250x). These were chosen for use as a reference only if they appeared to lie flat on the substrate, with at least 15 μm of gauge length parallel to the stress axis within a grain. A map of the location of each was made using an XY stage on the optical microscope which was then transferred to another map compatible with the XY stage of the SEM. This facilitated the rapid location of the chosen measurement sites in the SEM. The grain size at a measurement site was determined from the optical micrographs.

Flexural loading through the tensile half loading cycle was done in the SEM using the jig pictured in Fig. 10. A reversing drill connected to a rotary feedthrough into the SEM was used to operate the jig. Measurements were made at zero load to avoid tilting of the surface which could introduce error. To obtain the proper hysteresis loop, unloading in air after fatigue was completed through the compressive half cycle.

2.2.2 Microplasticity Results (ONR Funded Research)

Measured values of residual cyclic strain, ε, are given in Fig. 11 for Al 2219-T851, plotted as a function of the maximum slip distance to the grain boundaries measured through the center of the measurement site. As illustrated in Fig. 7, the maximum slip distance within the grain is measured at a 45° angle to the principal stress axis. Data are presented for two cases. The open circles are for a specimen cycled through a single half loading cycle with a peak surface stress of σ_{max} = 270 MPa (0.75 σ_{yield}). The residual strains for all grain sizes are indistinguishable from zero, indicating the material is purely elastic for the first tensile loading cycle.

We have found that, at least initially, values of ε in the larger grains progressively increase with fatigue. Tens of thousands of cycles are required to produce maximum values of ε in the largest grains in the alloy at σ_{max} = 270 MPa. Data after 20×10^3 fatigue cycles in dry air are given by the solid circles in Fig. 11. These clearly show a preference for ε to be largest in the larger grains, consistent with models proposed by Chang et al.,[19] and Tanaka and Mura[15] describing fatigue crack initiation. The strains

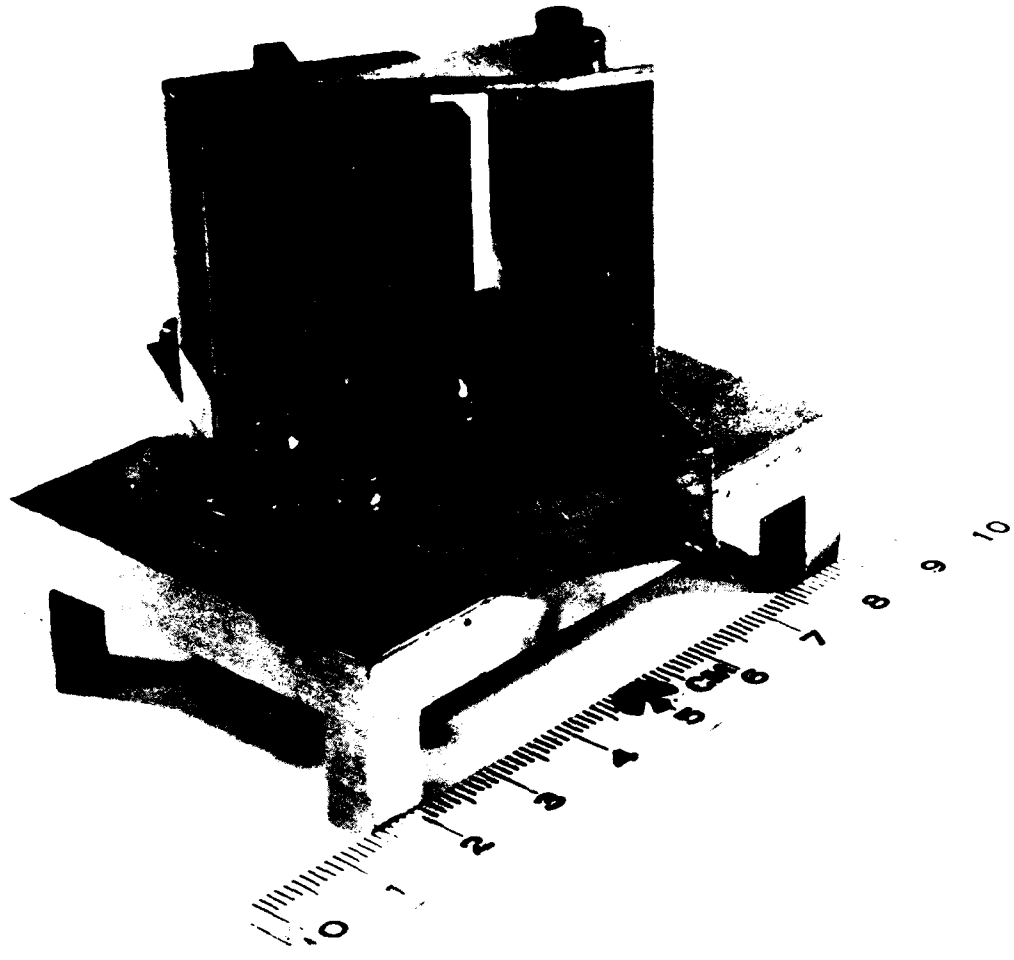

Fig. 10 Jig used to load a flexural fatigue specimen in the SEM. A reversing drill is connected through a rotary feedthrough into the microscope to the shaft A which moves the load bar B up or down along guide shafts via a worm gear. Surface stress on the specimen (C) is calibrated to the deflection of B, which is monitored by counting drill revolutions (typically 450 turns to yield). Data are taken from grains only within the region defined by the parallel lines.

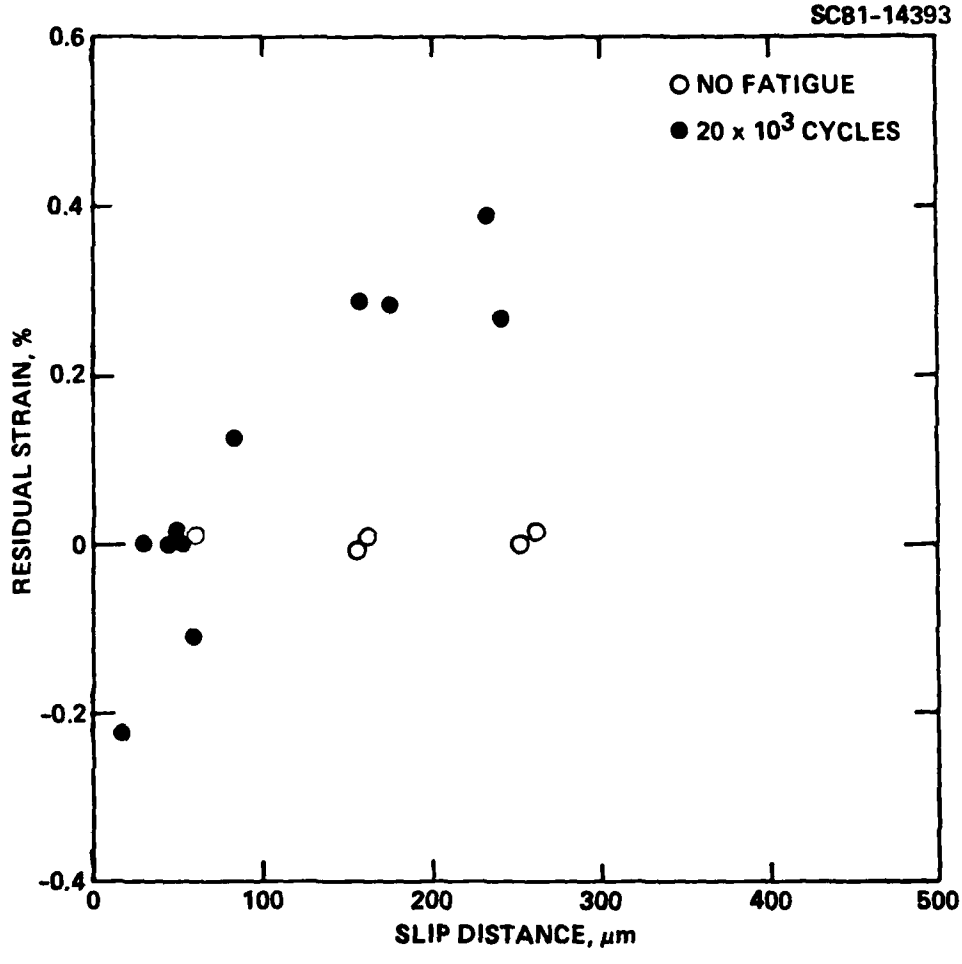

Fig. 11 Measured residual cyclic strain is plotted versus the maximum slip distance through the measurement site for two periods of fatigue. Data for Heat III in dry air. Open circles first tensile loading cycle. Closed circles after 20×10^3 cycles at ±270 MPa.

are quite large and must require that substantial redistribution of the local stresses within the neighboring grains occur to accommodate the fatigue induced microplasticity. For instance, small grains in which ε is negative are found to lie at the boundaries of large grains in which ε is positive. Apparently, a large grain yields in tension and, on unloading, imposes an elastic compression on itself and neighboring grains. Undoubtably, the true peak tensile plastic strain in the larger grains was larger than the measured ε.

The expected error in the measurement of ε is small compared to the observed scatter, which can be attributed to such factors as the variation of the grain's crystallographic orientation, the depth of the subsurface grain boundary, and the location of the measurement site within the grain. If we allow for a possible 0.2% compressive elastic strain reacting on the large grains, it appears likely that the peak localized tensile plastic strain in the surface may exceed 0.5% after 20×10^3 cycles. Thus, it is not surprising that surface constituent particles in Al 2219-T851 fracture in the larger grains in substantial numbers after such fatigue.[20] We believe these changes are localized near the surface. No opening of the stress-strain hysteresis loop was observed in axial fatigue of smooth bar specimens of Al 2219-T851 cycled at σ_{max} = 270 MPa, verifying that bulk plastic deformation did not take place.

Rockwell International funds have been used to study the effect of cyclic stress amplitude, fatigue cycles and pre-fatigue on the surface microplasticity of Heat III material fatigued in 50% relatively humidity air, so that a baseline model of the process can be developed. ONR funds have

supported studies of the effect of humidity and alloy hydrogen content (in either as-received or charged materials) on the development of microplasticity at the surface. While this work is still in progress, several interesting observations can be reported.

For comparison to the dry air data for Heat III in Fig. 11, we show in Figs. 12 and 13 results for Heats II and III at the same loading conditions but for fatigue in 50% relative humidity air. The peak plastic strains in Heat II in moist air are comparable to Heat III in dry air, even though the grain size is smaller in Heat II. The peak residual plastic strains are smaller for Heat III in moist than in dry air. We further find that with progressive fatigue at 5, 20 and 30 × 10^3 cycle increments, the residual plastic strains reach a peak within individual grains and then decrease with subsequent fatigue. The peak residual strain is larger and occurs at fewer cycles in the larger grains.

Our first attempt to measure residual plastic stains for a hydrogen charged Heat III material gave inclusive results. We had planned to fatigue the charged specimen for 20 × 10^3 cycles (lifetimes normally well exceed 30 × 10^3 at the amplitude used for the uncharged material). By 13 × 10^3 cycles the cracking density was already too large to continue, and even too large to make good residual plastic strain measurements. We were able to confirm that there were quite large residual compressive strains (< 0.2%) in some of the small grains of the specimen, but all the large grains contained cracks and no measurements could be taken there. The experiment is now being repeated for 5 × 10^3 cycles.

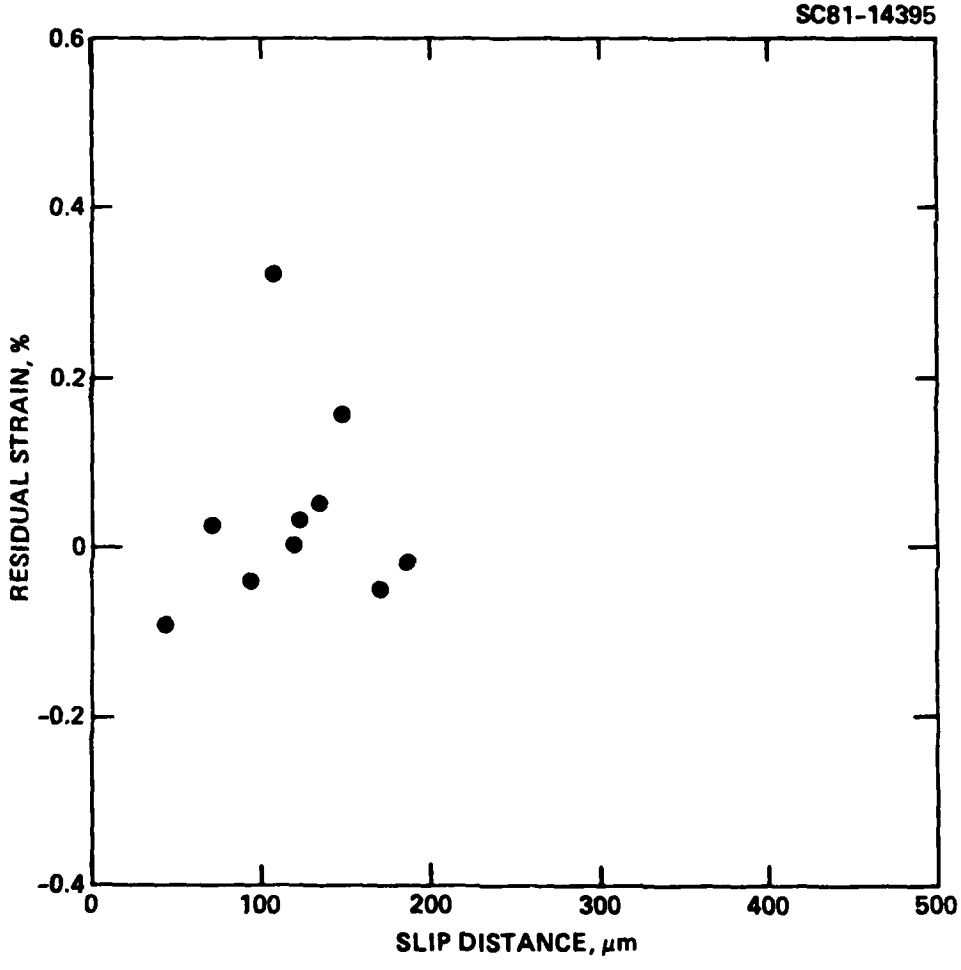

Fig. 12 Residual strain data for Heat II in 50% relative humidity air. Taken after 20×10^3 cycles at ±270 MPa.

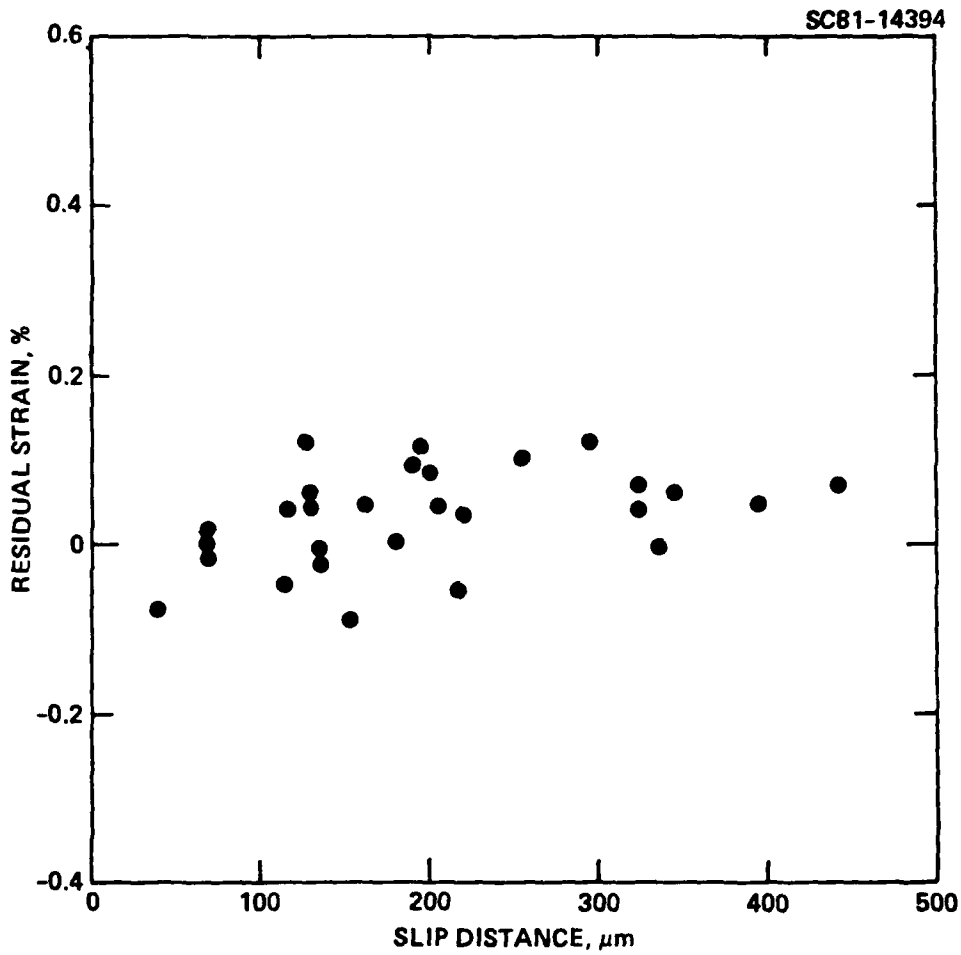

Fig. 13 Residual strain data for Heat III in 50% relative humidity air. Taken after 20×10^3 cycles at ±270 MPa.

2.3 Large Strain Ductility at Crack Tips

Large strain ductility behavior of the surface is obtained by measuring the crack tip deformation properties of microcracks at the alloy surface.[1] Values of parameters ε_y' for the three Al 2219-T851 alloys are given in Table 2. ε_y' is obtained by measuring the crack tip opening displacement (CTOD) of cracks at the surface, with appropriate normalization for the effect of crack length and grain size at the crack tip on CTOD as illustrated in Fig. 14. Numerous such measurements are required for each material to obtain reasonable accuracy. This methodology is described in more detail elsewhere.[1] An interesting trend in the effect of environmental humidity and internal hydrogen on ε_y' is found for two Al 2219-T851 alloys. The high hydrogen content (Heat II) material in both moist and dry air and the low hydrogen content material (Heat III) in moist air all have essentially the same ε_y' value. Only for the low hydrogen content alloy in dry air is ε_y' larger.

Table 2
Surface Ductility Parameters

Al 2219-T851 Heat	θ, Cycle^{-1}		ε_y'	
	Dry Air	Moist Air	Dry Air	Moist Air
I (Med. H, Low Fe)	-	-	0.16	0.26
II (High H, High Fe)	$<1 \times 10^{-6}$	$<1 \times 10^{-6}$	0.29	0.27
III (Low H, High Fe)	1×10^{-5}	3.5×10^{-5}	0.37	0.29

SC81-14396

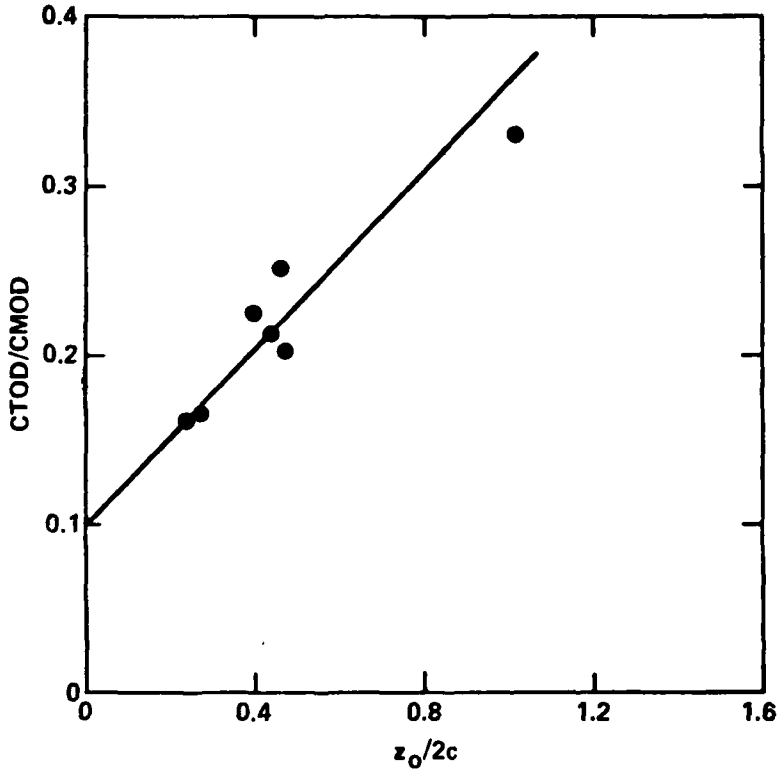

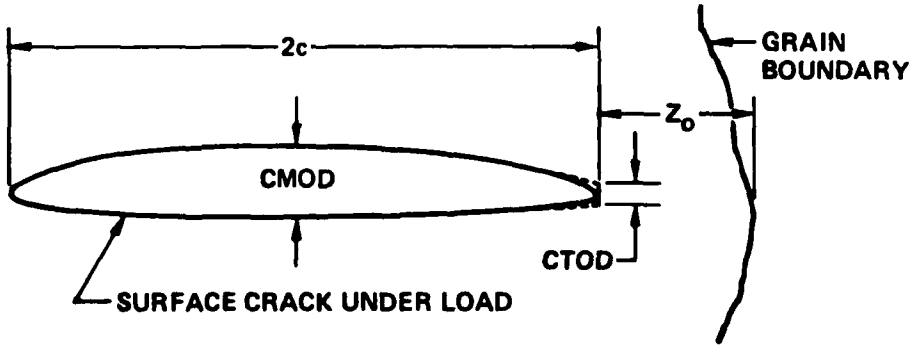

Fig. 14 CTOD data are plotted as a function of distance of the surface crack tip to the next grain boundary (z_0) to obtain parameter ε', which is larger if the material is more ductile, i.e., if the CTOD/CMOD ratio is larger. Shown are data for Heat I in dry air. See References 1 and 6 for more details on normalization. Below is schematic view of a crack of length 2c, illustrating geometric parameters plotted in figure.

For convenience, in comparison to ε_y', we have also listed experimental values of parameter θ in Table 2. This parameter describes one aspect of the cyclic hardening of the surface at small strains. Surfaces having larger values of θ harden more rapidly. This aspect of surface ductility is discussed more fully elsewhere.[20,21]

3.0 DISCUSSION

There are two aspects of our results which deserve discussion. One is the apparent duality of behavior of the mechanical properties of the surface of Al 2219-T851 at small plastic strain, wherein some observations suggest that the surface cyclicly hardens and others that it softens. The other results of special interest are observations which bear upon competing effects that influence surface ductility; these being the effects of hydrogen and of surface oxide at large and at small plastic strains.

3.1 Hardening vs Softening of the Surface of Al 2219-T851 at Cyclic Stress Amplitudes Less Than the Yield Strength

The mechanical properties of the surface of Al 2219-T851 are both sensitive to the ambient environment, and are distinctly different from the bulk properties. For instance, we find no measurable stress-strain hysteresis in smooth bars fatigued at amplitudes which produce measurable plastic strains at the surface. Indeed, the observation that small grains are driven into compression to compensate for tensile residual plastic strains in large grains illustrates the localized nature of the surface deformation.

Both Chang et al.,[19] and Tanka and Mura[15] have proposed models of fatigue crack initiation which ascribe to a surface grain localized plastic strains which increase progressively during fatigue. With the exception of a back stress, assumed proportional to dislocation density, these models ignore mechanisms which could both reduce the rate of accumulation of plastic strain,

and also reduce the peak values of the tensile plastic strain. We have extensively evaluated the Chang model by comparing predicted and measured rates of crack initiation in Al 2219-T851.[20] It substantially overestimates the numbers of constituent particles fractured for fully reversed loading at stress amplitudes sufficiently low to produce lifetime in excess of 20×10^3 cycles.

There is substantial evidence that this disparity is due to cyclic hardening of the surface. Apparently, one aspect of the hardening is a trend towards the surface deformation to become more homogeneous. This is manifested by a decreasing probability for the growth of small surface cracks to occur as crystallographic cracks, as the surface of the alloy is fatigued.

The average rate of propagation of small surface cracks across grain boundaries also decreases as the surface is fatigued. This is true for both crystallographic and for non-crystallographic growth into the new grain, and suggests that the hardening responsible for this change is more complex than a simple transition to more homogeneous slip, with concomitant suppression of reinitiation of the crack in the grain at the crack tip.

Thus cyclic hardening of the surface of the alloy is manifested in several ways with increasing fatigue: suppression of crack initiation; suppression of crack growth across grain boundaries; and by an increasing indentation hardness. For similar alloys Kramer[22] has reported an increase in the yield strength with fatigue at cyclic amplitudes below the yield strength. All these observations are consistent with cyclic hardening of the surface,

which begins at the first loading cycle and increases progressively with fatigue.

Our observations that the local yield stress of the matrix material within individual large grains initially decreases with fatigue are not contradictory with the body of evidence that the surface hardens. The degree of plasticity which can occur locally is a function of: (1) the density of new mobile dislocations induced by fatigue, which as shown by Pangborn et al.[18] may initially be small and ultimately, with fatigue, increased to an equilibrium value; and (2) the mobility of those dislocation, which can be presumed to decrease as the surface hardens. It is easy to imagine that indentation hardness, for instance, measures local dislocation mobility at large strains and is insensitive to the number of potentially mobile dislocations in a grain prior to indentation.

At least for Al 2219-T851, we are convinced that it is the localized plastic strain, and not progressive surface hardening as suggested by others which gives rise to crack initiation. We find that this plasticity is larger and develops more rapidly in specimens apparently rich in internal hydrogen, and in specimens having little internal hydrogen if they are fatigued in dry air (see Section 3.2). When this effect was originally detected indirectly, we suggested that the effect of hydrogen was to reduce the rate of cyclic hardening of this surface; because at high stress amplitudes, where hardening has the least effect, the rates of fracture of constituent particles is insensitive to alloy hydrogen content. However, our conclusion presupposes that hydrogen does not simultaneously effect the fracture strengths of the

constituent particles. Microscopic residual strain measurements as a function of hydrogen content and cyclic stress amplitude should unambigously determine if the effect of hydrogen in Al 2219-T851 at small strains is to reduce the rate of cyclic hardening, or to increase the rate of production of mobile dislocations for a fixed value of local cyclic stress.

3.2 Competitive Effect of Surface Oxide and Hydrogen on Surface Ductility

An analytic theory of the simultaneous effect of hydrogen and of surface oxide on the ductility of the surface of aluminum still eludes us. The Chang[19] model of crack initiation at particles, appropriately modified to deal with surface hardening, does provide useful predictions; but when looked at carefully in the light of our recent data it is clearly at best an approximation.[20] The peak tensile strain does not saturate at an equilibrium value as this theory predicts, but instead proceeds through a peak and returns to zero. Empirical models can be constructed which mimic this behavior. The simplest is to equate the peak residual strain to a product of the mobile dislocation density and of a local stress range given by the difference of the peak applied stress and a local short range stress (which increases as the surface hardens). We have, in fact, made such a construction, and found that not all our observations can be reproduced unless a complex empirical law of cyclic hardening is assumed. We see no point in proceeding further along this line until additional experimental data is obtained, on the effect of hydrogen on the cyclic hardening process.

However, we have a partial explanation for the diversity of our observations on the effect of hydrogen and of atmospheric humidity on surface ductility of Al 2219-T851. These are summarized qualitatively (in terms of low or high ductility) in Table 3. Two apparently anomalous results are inscribed in brackets and are rationalized as follows. Hydrogen results in a lowered ductility and a more rapid crack growth, and may come from internal sources or from an external source such as from the oxidation of freshly exposed aluminum by water vapor. This mechanism has also been proposed by Bowles[23] to explain his recent observation of the effect of humidity on CTOD in Al 2024-T3. Thus, the high ductility of Heat III in dry air can be attributed to the absence of hydrogen from either an internal or external source. At small plastic strains, such as are encountered before a crack forms, the amount of hydrogen which transits the surface oxide is small in humid air. Hydrogen maintains the ductility at small strains of aluminums rich in internal hydrogen. In a material poor in internal hydrogen, dislocation tangles form underneath the surface oxide as described by Grosskreutz,[2] and accelerate cyclic hardening, resulting in less microplastic strain. Thus using this rationale the surface ductility of Heat III in humid air is low, because no hydrogen is available to suppress hardening which is associated with a tendancy for dislocation tangles to form under the surface oxide layer. We hope that continued research along the present lines will lead to an analytic description of these processes.

Table 3

Qualitative Evaluation of Surface Ductility

Heat		Crack Initiation		Crack Growth	
		0% RH*	50% RH	0% RH	50% RH
II	High Hydrogen	High	High	Low	Low
III	Low Hydrogen	High	Low	High	Low

*RH - Relative humidity

4.0 SUMMARY

Our results are as follows:

1. Our measurements of the surface ductility of the matrix of Al 2219-T851 is divided into two regimes: (a) small plastic surface strains induced by fatigue which leads to crack initiation; (b) large plastic strains associated with the growth of surface crack tips.

2. Because the measurements are microscopic, as well as at the surface, we assess only the ductility of the matrix material. Less localized measurements might also include integrated effects of environment on grain boundaries and on constituent particles which could mask the fundamental changes of interest.

4.1 Small Plastic Strains

3. A technique is described to measure residual strains sustained for a tensile loading cycle, within individual grains at the surface. This involves the use of flakes of mica on the surface which serve as a reference against which small (20 Å) displacements in the surface can be measured.

4. Fatigue is done in fully reversed loading at a stress amplitude of 270 MPa. The surface is initially elastic and with increasing fatigue sustains progressively larger plastic strains under tensile loading. These are largest and develop more rapidly in the larger grains in the alloy. The largest values of localized plastic strain reached is less than 0.5%, and occurs only on a very small fraction of the surface area of the specimen within large grains. The average plasticity is too small to measure using a strain gauge.

5. The effect is localized at the surface, because smooth bar specimens fatigued for the same loading cycle show no stress-strain hysteresis measured axially. Furthermore, the degree of surface ductility is sensitive to atmospheric humidity.

6. Data were obtained for two heats of Al 2219-T851. Measured as-received internal hydrogen contents of these are less than 1 ppm, and so are not reliable. Qualitative comparison of the hydrogen content between the two heats was made by annealing the materials to form bubbles which were then counted. It appears from this that one material (denoted Heat II) is substantially richer in hydrogen than the other (denoted Heat III). We have been able to hydrogen charge Heat III material, which on subsequent annealing developed a density of bubbles exceeding

that in Heat II. The resulting properties of the charged material changed in a way which is consistent with the differences between Heats II and III. It thus appears that a principal difference between the two heats is their as received hydrogen content.

7. We have preliminary data on the effect of ambient humidity and of internal hydrogen on the development of localized plastic strains in 2219 during fatigue at cyclic stress amplitudes less than the yield strength. Hydrogen accelerates and increases the peak values of plastic strain attained for a given number of fatigue cycles. The development of localized plasticity is more rapid in dry than in moist air in the hydrogen poor Heat III. Indirect evidence, obtained by counting broken constituent particles, indicates that humidity has no effect on the localized plasticity developed in the hydrogen rich Heat II material.

8. Heats II and III show simultaneous manifestation of cyclic hardening and softening. One concludes from indentation hardness data, and other indirect evidence, that the surface progressively hardens beginning from the first fatigue cycle when fatigued at amplitudes well below the bulk yield strengh. At the same time the peak plastic strains under tensile load are

initially zero, increase with fatigue, and ultimately at least in the largest grains return to near zero with extended fatigue. We rationalize this apparent contradiction by noting that the amount of localized plastic strain that will occur in a grain is a function both of the number of mobile dislocations which will support deformation, and of the hardness of the surface which determines the mobility of those dislocations. Indentation measures only mobility; localized plasticity initially increases as the number of mobile dislocations increases during fatigue.

9. Our working model is that the major effect of hydrogen, in acting to increase localized plasticity, is to slow the rate at which the surface cyclically hardens at small plastic strains. Furthermore, since hydrogen enhances ductility during initial fatigue, the decreases in ductility observed in humid air cannot be attributed to hydrogen. We favor the suggestion of Grosskreutz,[2] that the surface oxide formed in humid air decreases the ease of motion of dislocations through the surface resulting in tangles and an acceleration of near surface hardening. Our conclusion regarding the effect of hydrogen on cyclic hardening is tentative and will be subjected to rigorous testing for hydrogen charged materials.

4.2 Large Plastic Strains

10. The ductility of the matrix material at the surface for large plastic strains is determined by measuring the opening displacement (CTOD) of surface crack tips. This is done as a function of the location of the crack tips relative to the grain boundaries, so that we can account for the effect on CTOD of variations in plastic zone size with the distance of slip from the crack tip to the next grain boundary.

11. Normalized values of CTOD (referred to an ε_y') were obtained for three heats of Al 2219-T851. ε_y' is found to be smaller in materials containing large amounts of hydrogen, in the as-received state. Also, humidity has no effect on ε_y' for Heat II which is hydrogen rich. ε_y', in moist air in hydrogen poor Heat III is smaller than in dry air, and the same as Heat II in dry air. It therefore appears that, at large strains, hydrogen reduces the ductility of the matrix. The hydrogen apparently can be extracted from humid air as well as come from an internal source. We think it likely the hydrogen from external sources may cross the surface oxide barrier only at large strains, explaining the absence of an effect of external hydrogen on the microplasticity of the matrix before cracks initiate.

5.0 REFERENCES

1. W. L. Morris, M. R. James, O. Buck, R. Chang and J. W. Wert: Mechanisms by Which Humidity Alter Ductility, technical report on Contract No. C0014-79-C-0334, for period April 15, 1979 through April 14, 1980. Sponsored by the Office of Naval Research.

2. J. S. Grosskreutz: Surface Sci. 8, (1967), p. 173.

3. R. K. Viswanadham, T. S. Sun and J. A. S. Green: Corrosion, 36, (1980), p. 275.

4. D. Hardwick, M. Taheri, A. W. Thompson and I. M. Bernstein: "Hydrogen Embrittlement in a 2000 Series Aluminum Alloy," presented at the 109th AIME Annual Meeting, Feb. 24-28, 1980, Las Vegas, Nevada.

5. W. L. Morris and M. R. James: Met. Trans. A. 11, (1980), p. 850.

6. W. L. Morris: Met. Trans. A. 11, (1980), p. 117.

7. W. L. Morris, M. R. James and O. Buck: Eng. Fract. Mech, 13, (1980), p. 213.

8. R.A.H. Edwards and E. Eichenaues: Scripta Met. 14 (1980), p. 971.

9. D.E.J. Talbot and D.A. Granger: J. Int. Met. 92, (1963), p. 290.

10. Abdelfatouh Elkholy, Jocques Galland, Pierre Axoce and Paul Bastien: C.R. Acod. Sc. Paris. 284, (1977), p. 363.

11. R.W. Landgraf: in Work Hardening in Tension and Fatigue, 1977 AIME, New York, A.W. Thompson, Editor, p. 224.

12. W. L. Morris, M. R. James, and O. Buck: Met. Trans. 12A (1981), p. 57.

13. S. Taira, K. Tanaka and Y. Nakai: Mech. Res. Comm. 5 (1978), p. 375.

14. W. L. Morris and M. R. James: Met. Trans. 11A (1980) 850.

15. K. Tanaka and T. Mura: "A Theory of Fatigue Crack Initiation at Inclusions," submitted to Met. Trans.

16. D. L. Davidson and J. Lankford: Trans. ASME-J. Eng. Matls. and Tech. 98H (1976), p. 24.

17. D. R. Williams, D. L. Davidson and J. Lankford: Expt. Mech. 20 (1980), p. 134.

18. R. N. Pangborn, S. Weissman and I. R. Kramer: Met. Trans. 12A (1981), p. 109.

19. R. Chang, W. L. Morris and O. Buck: Scripta Met. 13 (1979), p. 191.

20. M. R. James and W. L. Morris: "Quantitative Modeling of Fatigue Crack Initiation," submitted to Matls. Sci. and Eng.

21. W. L. Morris, M. R. James and O. Buck: in Nondestructive Evaluation: Microstructural Characterization and Reliability Strategies, Trans-AIME, Warrendale, Pennsylvania, O. Buck and S.M. Wolf, Editors (1981), p. 387.

22. I.R. Kramer: Trans. TMS-AIME 230 (1964), p. 991.

23. C.O. Bowles: "Fatigue Crack Growth in Aluminum Alloys," Ph.D. Thesis, August 1978, Delft University of Technology, Netherlands.

END

DATE
FILMED
11-81

DTIC